

Biased Teacher, Balanced Student

Seonghak Kim

Abstract—Knowledge Distillation (KD) is a widely adopted model compression technique where a compact student model learns from the output of a larger, pre-trained teacher. While effective in balanced settings, conventional KD suffers significantly when applied to long-tailed data distributions, as the teacher model tends to be biased toward head classes and provides limited supervision for tail classes. In this paper, we propose Long-Tailed Knowledge Distillation (LTKD), a novel framework tailored for class-imbalanced scenarios. We begin by reformulating the standard KD objective into two components: inter-group and intra-group Kullback–Leibler (KL) divergence, corresponding to the prediction distributions across and within class groups (head, medium, tail), respectively. This decomposition allows us to identify and quantify the sources of teacher bias. To address them, we introduce (1) a rebalanced inter-group loss that calibrates the teacher’s group-level predictions and (2) a uniform intra-group loss that ensures equal contribution from all groups during distillation. Extensive experiments on CIFAR-100-LT, TinyImageNet-LT, and ImageNet-LT show that LTKD consistently outperforms existing KD methods, achieving significant gains in both overall accuracy and tail-class performance. Our results demonstrate that LTKD enables effective knowledge transfer even from biased teachers, making it a strong candidate for real-world deployment in resource-constrained and imbalanced settings.

Index Terms—Knowledge Distillation, Long-Tailed Distribution, Class Imbalance, Model Compression, Inter-group and Intra-group KL Divergence, Teacher Bias Correction

I. INTRODUCTION

DEEP learning has achieved remarkable performance across a wide range of computer vision tasks, including image classification [1]–[3], object detection [4], [5], semantic segmentation [6]–[8], panoptic recognition [9], [10], and multimodal fusion [11], [12]. These successes are largely attributed to high-capacity neural network architectures with billions of parameters and deep hierarchical structures. While such large-scale models offer high accuracy, they also demand substantial computational and memory resources, making them challenging to deploy in resource-constrained environments such as edge devices and real-time systems commonly used in industrial and autonomous driving applications. To address these practical limitations, various model compression techniques—such as pruning [13], quantization [14], and knowledge distillation (KD) [15]—have been proposed.

Among them, KD is a highly promising compression technique in which a compact student network is trained to mimic the behavior of a larger teacher network. In the original KD paradigm introduced by Hinton [16], the teacher and student are trained on a balanced dataset [17], [18], and the student

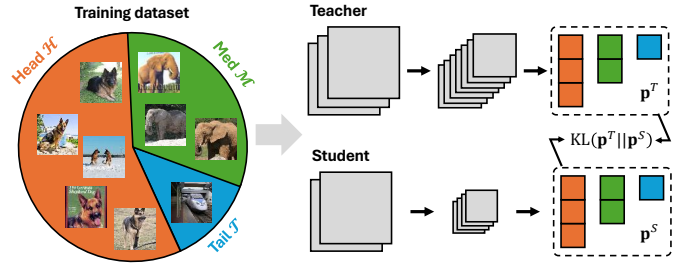


Fig. 1: Overview of standard KD under long-tailed distributions. The training data exhibit severe class imbalance, as illustrated by the pie chart, where most samples belong to head classes (orange) and only a few to tail classes (blue). The teacher, trained on such data, becomes biased and produces predictions (p^T) that overemphasize head classes. When KD is applied, the student mimics this biased distribution (p^S), resulting in poor generalization on tail classes.

learns not only from ground-truth labels but also from the teacher’s softened output probabilities (i.e., logit-based KD) or internal feature representations (i.e., feature-based KD). Since its introduction, most logit-based KD methods [16], [19] have been formulated as minimizing the Kullback-Leibler (KL) divergence between the softened output distributions of the teacher and the student. Under the assumption of balanced data, the teacher provides reliable guidance across all classes, allowing the student to approach the teacher’s performance with far fewer parameters.

However, as shown in Fig. 1, real-world datasets typically follow a long-tailed distribution, where the majority of samples belong to a few head classes and only a limited number of samples represent the tail classes [20]. In such scenarios, the assumption of balanced data breaks down. When trained on long-tailed data, the teacher network becomes biased toward the head classes—it performs well on frequent classes but poorly on rare ones due to insufficient exposure. As a result, applying standard KD directly in this context becomes ineffective: the student inherits the teacher’s biased knowledge and struggles particularly with tail classes. Empirical studies confirm that standard KD disproportionately emphasizes head-class predictions while offering little informative guidance for tail-class samples. Consequently, there is a pressing need for KD methods that remain effective under long-tailed data distributions, enabling students to learn balanced knowledge even from biased teachers.

To address this, as shown in Fig. 2, we propose *Long-Tailed Knowledge Distillation (LTKD)*—a novel distillation approach tailored for class-imbalanced scenarios. We begin by reformulating the traditional KL-based KD objective into

Seonghak Kim is with the Agency for Defense Development (ADD), Daejeon 34186, Republic of Korea (e-mail: seonghak35@gmail.com).

This work has been submitted to the IEEE for possible publication. Copyright may be transferred without notice, after which this version may no longer be accessible.

two components: an inter-group term and an intra-group term, enabling us to analyze how knowledge is transferred from teacher to student in the presence of long-tailed data. By defining appropriate class groups (e.g., head, medium, and tail), we show that the inter-group term reflects mismatches in aggregated prediction probabilities across different groups, while the intra-group term captures discrepancies within each group. Our theoretical and empirical analyses reveal that these two terms expose distinct signs of teacher bias. The inter-group term significantly contributes to overestimating head-class predictions and underestimating tail-class predictions, as it operates on aggregated probabilities. The intra-group term, due to being weighted by the group’s aggregate predictions, tends to effectively transmit head-group signals while largely neglecting tail-group signals.

Building on this insight, we introduce a rebalancing strategy that adjusts the contribution of the inter- and intra-group terms. This rebalancing ensures that information from all class groups is equally conveyed to the student, effectively compensating for the teacher’s skewed emphasis. Intuitively, this approach offsets the distortion introduced by class frequency and enables the student to learn a more balanced representation.

In summary, our contributions are threefold:

- We derive a novel decomposition of the KD objective into inter-group and intra-group loss components.
- We demonstrate that each component includes distinct aspects of teacher bias arising from long-tailed training data.
- We propose a rebalanced distillation method that utilizes this decomposition to train a balanced student, capable of surpassing the teacher’s performance, particularly on tail classes.

We validate our proposed LTKD method on standard long-tailed benchmarks for image classification: CIFAR-100-LT [21], TinyImageNet-LT, and ImageNet-LT [22], all of which exhibit severe class imbalance. Experimental results show that LTKD consistently outperforms state-of-the-art methods on these datasets. Notably, our method achieves substantial improvements on tail classes, even surpassing the teacher’s performance. These results underscore the effectiveness of LTKD in transferring knowledge from a biased teacher to a compact student, marking a significant step toward deploying high-performance models in real-world scenarios with imbalanced data.

II. RELATED WORKS

A. Conventional Knowledge Distillation

Knowledge distillation (KD) is a widely adopted paradigm for transferring knowledge from a large, accurate teacher model to a lightweight student model, aiming to preserve performance while reducing computational cost [15]. The central idea is to exploit the rich information—often referred to as dark knowledge [23]—present in the teacher’s outputs to guide the training of the student. Broadly, KD approaches fall into two categories: logit-based distillation and feature-based distillation, depending on whether the student learns from the teacher’s final predictions or internal representations.

In logit-based distillation, the student is trained to match the output distribution of the teacher, typically by minimizing the Kullback–Leibler (KL) divergence between their softmax probabilities [16]. Early methods such as Deep Mutual Learning (DML) introduced mutual supervision between models [24], while Teacher Assistant KD (TAKD) addressed capacity gaps by introducing an intermediate assistant model [25]. More recently, Decoupled KD (DKD) decomposed the soft label loss into target and non-target components, enabling more flexible guidance during training [19].

Meanwhile, feature-based distillation focuses on transferring internal knowledge from the teacher by aligning hidden representations. FitNet was among the first to utilize intermediate features, encouraging the student to learn not just final predictions but also internal structures [26]. This idea was extended by methods such as Attention Transfer (AT), which aligned spatial attention maps [27]; Relational KD (RKD), which captured sample-wise relational information [28]; and Contrastive Representation Distillation (CRD), which reformulated feature transfer as a contrastive objective [29]. ReviewKD further advanced this line of research by integrating a residual-style fusion of earlier feature layers to guide later ones more effectively [30].

Despite their effectiveness, most existing KD methods assume a balanced class distribution in the training data, where each class has a similar number of samples [31]–[35]. However, real-world datasets often follow a long-tailed distribution, where head classes dominate the data and tail classes are severely underrepresented [36]. When a teacher model is trained under such an imbalanced setting, it tends to focus disproportionately on frequent (head) classes, introducing an implicit bias in its predictions. Applying standard KD in this context causes the student to inherit this bias, resulting in poor generalization on rare classes and reduced overall robustness.

To address the limitations of conventional KD in long-tailed settings, we propose a novel approach that explicitly accounts for class imbalance. We first reformulate the KL divergence loss into two components: inter-group KL, representing the distribution over head, medium, and tail class groups, and intra-group KL, reflecting the distribution within each group. Both components are shown to be affected by the teacher’s bias toward head classes. To mitigate this, we apply a dual rebalancing strategy: we calibrate the inter-group distribution to reduce head-class dominance and uniformly reweight the intra-group terms to ensure fair supervision across all class groups. This allows the student to learn from a recalibrated teacher, resulting in more balanced and effective knowledge transfer. Unlike prior works that assume balanced data or ignore teacher bias, our method is tailored for real-world long-tailed scenarios and achieves outstanding performance, especially on underrepresented classes.

B. Knowledge Distillation in Long-Tailed Distribution

Recent efforts have explored knowledge distillation (KD) under long-tailed class distributions, where the imbalance in training data leads to biased teacher predictions. A straightforward approach in this setting is to modify the distillation objective to account for class imbalance. For instance,

Balanced Knowledge Distillation (BKD) proposes a dual-loss framework that combines an instance-balanced classification loss with a class-balanced distillation loss, aiming to enhance performance on underrepresented classes [37]. However, these methods typically assume that the student has a capacity similar to the teacher. In many cases, the student is essentially a replica of the teacher architecture, retrained with balanced supervision. As a result, the primary goal becomes improving classification accuracy—particularly for tail classes—rather than reducing model size.

Another notable direction involves multi-teacher distillation. For example, Learning From Multiple Experts (LFME) introduces a self-paced framework that aggregates knowledge from multiple expert models, each trained on less imbalanced subsets of the data [38]. Through adaptive selection of both experts and samples, LFME improves generalization in long-tailed scenarios. However, the resulting student models are typically on par with the teacher models. Once again, the focus remains on classification accuracy rather than model compression.

In summary, while prior works [37], [38] have made progress in adapting KD to class-imbalanced scenarios, they generally assume that the student model retains most of the teacher’s capacity. Consequently, these approaches are less about compression and more about refining performance on skewed datasets.

In contrast, our work is grounded in model compression. We aim to distill knowledge from a biased teacher into a significantly smaller student, suitable for deployment in resource-constrained environments. This setting presents unique challenges, as the student not only generalize well from limited capacity but also avoid inheriting the teacher’s bias toward head classes.

To address this, we propose Long-Tailed Knowledge Distillation (LTKD), which explicitly decomposes the standard KL divergence loss into inter-group and intra-group components. We identify that both components are affected by the teacher’s class imbalance, and we apply a rebalancing strategy to correct for this bias. By doing so, the student receives balanced supervision even from a skewed teacher, allowing it to achieve strong performance—especially the tail—while maintaining a compact model size.

III. METHOD

In this section, we take a closer look at the mechanism of knowledge distillation. Since our focus is on the long-tailed distribution problem, we decompose the KD loss into head, medium, and tail components based on the class distribution, and show that the KD loss can be expressed as a weighted sum of these elements. By analyzing the contribution of each component, we reveal the limitations of logit-based methods such as conventional KD [16] and DKD [19], which are grounded in KL divergence. Motivated by these findings, we propose a novel knowledge distillation method that overcomes these limitations and extracts relatively balanced knowledge from a teacher trained under a long-tailed scenario.

A. Revisiting KD under Long-Tailed Distribution

In a classification task where a sample \mathbf{x} is categorized into one of C classes, the predictive probability vector is represented as $\mathbf{p} = [p_1, p_2, \dots, p_C] \in \mathbb{R}^C$, which is obtained by applying the softmax function $\sigma(\cdot)$ to the logit vector $\mathbf{z} = [z_1, z_2, \dots, z_C] \in \mathbb{R}^C$ as follows:

$$p_i = \sigma(z_i) = \frac{\exp(z_i)}{\sum_{j=1}^C \exp(z_j)},$$

where p_i and z_i denote the probability and logit value corresponding to the i -th class, respectively.

Since we assume that the dataset follows a long-tailed distribution, we divide the overall probability distribution into head, medium, and tail class distributions. Specifically, the entire dataset \mathcal{D} is partitioned into three groups $\mathcal{G} \in \{\mathcal{H}, \mathcal{M}, \mathcal{T}\}$, such that $\mathcal{D} = \mathcal{H} \cup \mathcal{M} \cup \mathcal{T}$, and the groups are mutually disjoint.

Accordingly, conventional KD, which uses Kullback–Leibler (KL) divergence as its loss function, can be formulated as follows:

$$\begin{aligned} \text{KD} &= \text{KL}(\mathbf{p}^T \| \mathbf{p}^S) \\ &= \sum_{i=1}^C p_i^T \log \left(\frac{p_i^T}{p_i^S} \right) \\ &= \sum_{\mathcal{G}} \sum_{i \in \mathcal{G}} p_i^T \log \left(\frac{p_i^T}{p_i^S} \right), \end{aligned}$$

where the teacher and student models are denoted by T and S , respectively.

To proceed with the formulation, we introduce two new notations. The first is $\mathbf{p}_{\mathcal{G}} = [p_{\mathcal{H}}, p_{\mathcal{M}}, p_{\mathcal{T}}] \in \mathbb{R}^3$, where each element represents the aggregated probability over the head, medium, and tail class groups, respectively. We refer to this as the inter-group probability distribution, defined as:

$$p_{\mathcal{G}} = \frac{\sum_{i \in \mathcal{G}} \exp(z_i)}{\sum_{j=1}^C \exp(z_j)}.$$

The second notation is $\tilde{\mathbf{p}}_{\mathcal{G}} = [\tilde{p}_{\mathcal{G}_1}, \tilde{p}_{\mathcal{G}_2}, \dots, \tilde{p}_{\mathcal{G}_i}]_{i \in \mathcal{G}} \in \mathbb{R}^{|\mathcal{G}|}$, which defines the probability distribution within each class group. We refer to this as the intra-group probability distribution, calculated as:

$$\tilde{p}_{\mathcal{G}_i} = \frac{\exp(z_i)}{\sum_{j \in \mathcal{G}} \exp(z_j)}.$$

Using the relationship between p_i , $p_{\mathcal{G}}$, and $\tilde{p}_{\mathcal{G}_i}$, we can rewrite p_i in the KD formulation as a product of inter-group and intra-group probabilities: $p_i = p_{\mathcal{G}} \cdot \tilde{p}_{\mathcal{G}_i}$. Based on this, the KD loss can be reformulated as:

$$\begin{aligned} \text{KD} &= \sum_{\mathcal{G}} \sum_{i \in \mathcal{G}} p_i^T \log \left(\frac{p_{\mathcal{G}}^T \tilde{p}_{\mathcal{G}_i}^T}{p_{\mathcal{G}}^S \tilde{p}_{\mathcal{G}_i}^S} \right) \\ &= \sum_{\mathcal{G}} \sum_{i \in \mathcal{G}} p_i^T \left(\log \frac{p_{\mathcal{G}}^T}{p_{\mathcal{G}}^S} + \log \frac{\tilde{p}_{\mathcal{G}_i}^T}{\tilde{p}_{\mathcal{G}_i}^S} \right) \\ &= \sum_{\mathcal{G}} \sum_{i \in \mathcal{G}} p_i^T \log \left(\frac{p_{\mathcal{G}}^T}{p_{\mathcal{G}}^S} \right) + \sum_{\mathcal{G}} \sum_{i \in \mathcal{G}} p_i^T \log \left(\frac{\tilde{p}_{\mathcal{G}_i}^T}{\tilde{p}_{\mathcal{G}_i}^S} \right). \end{aligned}$$

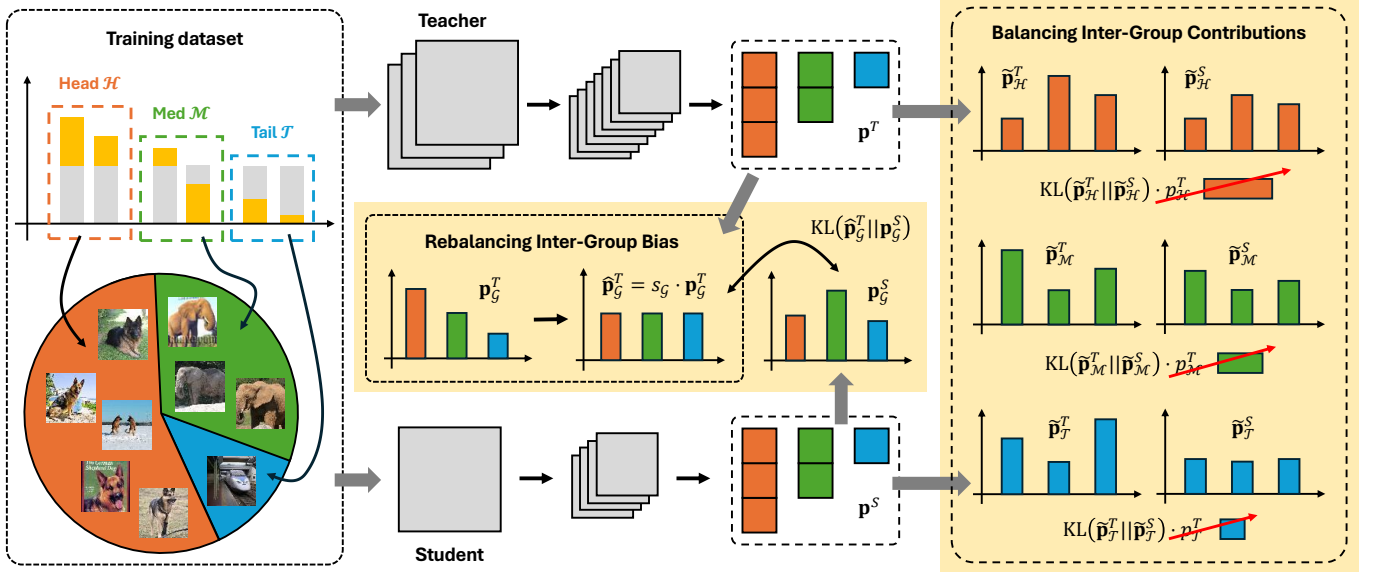


Fig. 2: Overview of the proposed Long-Tailed Knowledge Distillation (LTKD). We first decompose the standard KL-based KD loss into inter-group and intra-group components based on head, medium, and tail class groupings. The inter-group term reflects mismatches in aggregated group-level predictions, while the intra-group term captures within-group discrepancies. To correct the teacher’s class bias, we apply a rebalancing strategy that adjusts the contribution of each group, ensuring balanced knowledge transfer to the student.

Since both $p_{\mathcal{G}}^T$ and $p_{\mathcal{G}}^S$ are independent of the class index i , and $\sum_{i \in \mathcal{G}} p_i^T = p_{\mathcal{G}}^T$, the first term can be simplified as follows:

$$\begin{aligned} \sum_{\mathcal{G}} \sum_{i \in \mathcal{G}} p_i^T \log \left(\frac{p_{\mathcal{G}}^T}{p_{\mathcal{G}}^S} \right) &= \sum_{\mathcal{G}} p_{\mathcal{G}}^T \log \left(\frac{p_{\mathcal{G}}^T}{p_{\mathcal{G}}^S} \right) \\ &= \text{KL}(\mathbf{p}_{\mathcal{G}}^T || \mathbf{p}_{\mathcal{G}}^S), \end{aligned}$$

where $\mathbf{p}_{\mathcal{G}}^T = [p_{\mathcal{H}}^T, p_{\mathcal{M}}^T, p_{\mathcal{T}}^T]$ and $\mathbf{p}_{\mathcal{G}}^S = [p_{\mathcal{H}}^S, p_{\mathcal{M}}^S, p_{\mathcal{T}}^S]$ denote the inter-group probability distributions of the teacher and student, respectively.

Analogously, by using the relationship $p_i^T = p_{\mathcal{G}}^T \cdot \tilde{p}_{\mathcal{G}_i}^T$, the second term can also be simplified as follows:

$$\begin{aligned} \sum_{\mathcal{G}} \sum_{i \in \mathcal{G}} p_i^T \log \left(\frac{\tilde{p}_{\mathcal{G}_i}^T}{\tilde{p}_{\mathcal{G}_i}^S} \right) &= \sum_{\mathcal{G}} p_{\mathcal{G}}^T \sum_{i \in \mathcal{G}} \tilde{p}_{\mathcal{G}_i}^T \log \left(\frac{\tilde{p}_{\mathcal{G}_i}^T}{\tilde{p}_{\mathcal{G}_i}^S} \right) \\ &= \sum_{\mathcal{G}} p_{\mathcal{G}}^T \cdot \text{KL}(\tilde{\mathbf{p}}_{\mathcal{G}}^T || \tilde{\mathbf{p}}_{\mathcal{G}}^S), \end{aligned}$$

where $\tilde{\mathbf{p}}_{\mathcal{G}}^T$ and $\tilde{\mathbf{p}}_{\mathcal{G}}^S$ denote the intra-group probability distributions of the teacher and student for group \mathcal{G} , respectively.

Finally, the overall KD loss can be expressed as the sum of inter-group and intra-group KL terms:

$$\begin{aligned} \text{KD} &= \text{KL}(\mathbf{p}^T || \mathbf{p}^S) \\ &= \text{KL}(\mathbf{p}_{\mathcal{G}}^T || \mathbf{p}_{\mathcal{G}}^S) + \sum_{\mathcal{G}} p_{\mathcal{G}}^T \cdot \text{KL}(\tilde{\mathbf{p}}_{\mathcal{G}}^T || \tilde{\mathbf{p}}_{\mathcal{G}}^S) \\ &= \text{KL}(\mathbf{p}_{\mathcal{G}}^T || \mathbf{p}_{\mathcal{G}}^S) + p_{\mathcal{H}}^T \cdot \text{KL}(\tilde{\mathbf{p}}_{\mathcal{H}}^T || \tilde{\mathbf{p}}_{\mathcal{H}}^S) \\ &\quad + p_{\mathcal{M}}^T \cdot \text{KL}(\tilde{\mathbf{p}}_{\mathcal{M}}^T || \tilde{\mathbf{p}}_{\mathcal{M}}^S) + p_{\mathcal{T}}^T \cdot \text{KL}(\tilde{\mathbf{p}}_{\mathcal{T}}^T || \tilde{\mathbf{p}}_{\mathcal{T}}^S). \end{aligned}$$

The final formulation shows that the overall KD loss consists of two components: (1) a loss that aligns the inter-group probability distributions—i.e., the aggregated probabilities over head, medium, and tail classes—between the teacher

and student models, and (2) a loss that aligns the intra-group probability distributions within each of the three class groups. Notably, each intra-group KL term is weighted by $p_{\mathcal{G}}^T$, the inter-group probability of the teacher model, reflecting the relative importance of each group. This decomposition enables an analysis of the respective contributions of inter-group and intra-group learning under long-tailed distributions, and further reveals the limitations of conventional KL divergence-based methods.

It is worth noting that our formulation can be viewed as a generalized form of DKD. Specifically, when the class groups are simplified into just two categories — target and non-target — the formulation naturally reduces to the decoupled form introduced in DKD.

B. Rebalancing Inter-Group Bias

In long-tailed classification scenarios, a teacher model trained on an imbalanced dataset naturally exhibits prediction bias toward head classes, which dominate the data distribution. To examine this phenomenon, we analyze the inter-group output probabilities of a pre-trained teacher model $\mathbf{p}_{\mathcal{G}}^T = [p_{\mathcal{H}}^T, p_{\mathcal{M}}^T, p_{\mathcal{T}}^T]$ on both the balanced and long-tailed versions of CIFAR-100.

Specifically, we measure the sum of prediction probabilities for each class group—head, medium, and tail—within a single batch. On a representative batch from the balanced dataset, the teacher model produces nearly uniform group-wise predictions, with values of [22.54, 20.76, 20.70]. In contrast, the same analysis on a batch from the long-tailed dataset yields skewed outputs: [27.88, 19.28, 16.83], showing a clear bias toward the head group. This trend remains consistent across

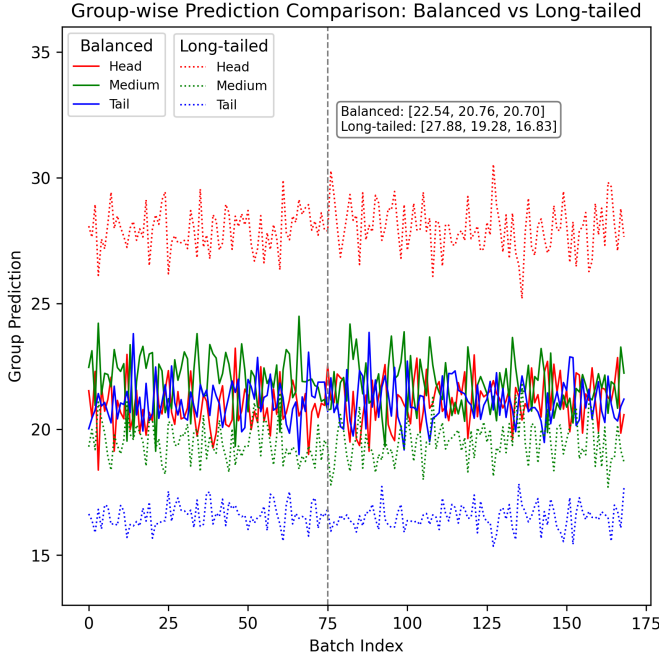


Fig. 3: Group-wise prediction trends of the teacher model on the CIFAR-100 dataset across training batches. On the balanced version (solid lines), the teacher produces nearly uniform group-wise outputs. In contrast, on the long-tailed version (dotted lines), the teacher assigns higher probabilities to head classes and lower probabilities to tail classes.

batches within a single epoch (see Fig. 3), indicating that the teacher model systematically assigns higher confidence to head classes.

This imbalance poses a key challenge in knowledge distillation. The KL-based distillation loss encourages the student model to match the teacher’s output, thereby inheriting the teacher’s head-biased predictions. Consequently, the student becomes further biased toward dominant classes, which can be detrimental to tail-class performance.

To mitigate this issue, we introduce a group-wise rebalancing mechanism that adjusts the teacher’s inter-group probability distribution before distillation. The goal is to align the sum of group-wise probabilities to a uniform distribution—e.g., [21, 21, 21]—instead of the skewed values observed under long-tailed settings. This is achieved by computing scaling factors for each group such that their reweighted predictions become equal across a batch.

Let the sum of inter-group probabilities in a batch B be $\mathbf{p}_{\text{sum}} = [p_{\mathcal{H}}^B, p_{\mathcal{M}}^B, p_{\mathcal{T}}^B]$. We define the target average as:

$$p_{\text{avg}}^B = \text{Mean}(p_{\mathcal{H}}^B, p_{\mathcal{M}}^B, p_{\mathcal{T}}^B),$$

and set the desired balanced vector as $[p_{\text{avg}}^B, p_{\text{avg}}^B, p_{\text{avg}}^B]$. The scaling factors for each group are then given by:

$$s_{\mathcal{H}} = \frac{p_{\text{avg}}^B}{p_{\mathcal{H}}^B}, s_{\mathcal{M}} = \frac{p_{\text{avg}}^B}{p_{\mathcal{M}}^B}, s_{\mathcal{T}} = \frac{p_{\text{avg}}^B}{p_{\mathcal{T}}^B}.$$

For each sample in the batch, we apply the appropriate scaling factor based on its class group:

$$\hat{\mathbf{p}}_{\mathcal{G}}^T = s_{\mathcal{G}} \cdot \mathbf{p}_{\mathcal{G}}^T.$$

This operation suppresses overrepresented groups and amplifies underrepresented ones, yielding a more balanced group-level distribution within each batch. However, this scaling process alone does not guarantee that the adjusted probabilities for each sample form a valid probability distribution, since:

$$\sum_{i=1}^C \hat{p}_i^T \neq 1.$$

To ensure proper normalization, we apply the following correction:

$$\hat{p}_i^T = \frac{s_{\mathcal{G}_i} \cdot p_i^T}{\sum_{j=1}^C s_{\mathcal{G}_i} \cdot p_j^T}.$$

This normalization step ensures that each prediction vector $\hat{\mathbf{p}}^T$ remains a valid probability distribution after rebalancing. Through this rebalancing, the student model is guided by a re-calibrated teacher that no longer disproportionately emphasizes the head group.

C. Balancing Intra-Group Contributions

As derived in Sec. III-A, the standard KL divergence between teacher and student predictions can be decomposed into two components: inter-group and intra-group losses. Here, we focus on the intra-group term, which can be written as a weighted sum of KL divergences within each group:

$$\begin{aligned} \sum_{\mathcal{G}} p_{\mathcal{G}}^T \cdot \text{KL}(\tilde{\mathbf{p}}_{\mathcal{G}}^T \| \tilde{\mathbf{p}}_{\mathcal{G}}^S) &= p_{\mathcal{H}}^T \cdot \text{KL}(\tilde{\mathbf{p}}_{\mathcal{H}}^T \| \tilde{\mathbf{p}}_{\mathcal{H}}^S) \\ &+ p_{\mathcal{M}}^T \cdot \text{KL}(\tilde{\mathbf{p}}_{\mathcal{M}}^T \| \tilde{\mathbf{p}}_{\mathcal{M}}^S) + p_{\mathcal{T}}^T \cdot \text{KL}(\tilde{\mathbf{p}}_{\mathcal{T}}^T \| \tilde{\mathbf{p}}_{\mathcal{T}}^S), \end{aligned}$$

where $\tilde{\mathbf{p}}_{\mathcal{G}}^T$ and $\tilde{\mathbf{p}}_{\mathcal{G}}^S$ are the intra-group distributions of the teacher and student, respectively, and $p_{\mathcal{G}}^T$ denotes the aggregated probability that the teacher assigns to group $\mathcal{G} \in \mathcal{H}, \mathcal{M}, \mathcal{T}$.

In long-tailed classification, due to the imbalanced nature of the training data, the teacher model tends to allocate higher prediction to head classes. This typically leads to a group-level ordering of $p_{\mathcal{H}}^T > p_{\mathcal{M}}^T > p_{\mathcal{T}}^T$. As a result, the intra-group KL loss becomes heavily biased toward the head group, while the contribution from the tail group is substantially diminished. This bias causes the student to receive weaker supervision signals for underrepresented classes, which limits its ability to generalize across the full label space.

To address this issue, we propose a reweighting strategy that enforces equal importance across all three groups, regardless of the teacher’s confidence. Specifically, we replace the teacher-derived weights $p_{\mathcal{G}}^T$ with a uniform constant, yielding the modified intra-group loss:

$$\begin{aligned} &\beta \cdot \sum_{\mathcal{G}} \text{KL}(\tilde{\mathbf{p}}_{\mathcal{G}}^T \| \tilde{\mathbf{p}}_{\mathcal{G}}^S) \\ &= \beta \cdot (\text{KL}(\tilde{\mathbf{p}}_{\mathcal{H}}^T \| \tilde{\mathbf{p}}_{\mathcal{H}}^S) + \text{KL}(\tilde{\mathbf{p}}_{\mathcal{M}}^T \| \tilde{\mathbf{p}}_{\mathcal{M}}^S) + \text{KL}(\tilde{\mathbf{p}}_{\mathcal{T}}^T \| \tilde{\mathbf{p}}_{\mathcal{T}}^S)), \end{aligned}$$

where β is a hyperparameter that controls the strength of the intra-group loss.

T-S Pairs	ResNet32×4 – ResNet8×4						VGG13 – VGG8					
γ Group	10		20		100		10		20		100	
	\mathcal{T}	All	\mathcal{T}	All	\mathcal{T}	All	\mathcal{T}	All	\mathcal{T}	All	\mathcal{T}	All
Teacher	50.72	64.95	39.19	58.82	15.28	45.35	45.67	60.77	36.43	55.10	14.01	43.11
Student	47.32	60.59	36.99	55.44	13.38	42.48	43.67	57.43	33.89	52.29	13.13	40.70
KD [16]	48.76	62.85	36.81	57.41	11.43	44.50	47.84	61.41	37.29	56.13	14.02	43.56
FitNet [26]	48.02	60.86	36.72	55.60	13.01	42.82	44.47	58.30	35.90	54.08	14.42	42.48
DKD [19]	49.86	64.55	37.87	58.78	13.25	46.11	48.00	61.84	37.65	56.68	14.42	44.22
ReviewKD [30]	52.08	64.71	40.12	59.17	15.09	45.91	47.75	61.43	37.69	56.51	14.76	44.19
LTKD	58.66	66.76	49.70	62.54	27.21	51.08	53.95	63.04	45.77	58.86	23.30	47.66
Δ	+6.58	+2.05	+9.58	+3.37	+12.12	+4.97	+5.95	+1.20	+8.08	+2.18	+8.54	+3.44

T-S Pairs	WRN-40-2 – WRN-40-1						ResNet110 – ResNet32					
γ Group	10		20		100		10		20		100	
	\mathcal{T}	All	\mathcal{T}	All	\mathcal{T}	All	\mathcal{T}	All	\mathcal{T}	All	\mathcal{T}	All
Teacher	49.77	63.05	39.88	58.27	14.88	44.78	47.28	61.18	36.63	55.49	13.32	42.45
Student	44.61	59.02	34.44	54.24	12.92	42.29	44.04	59.13	34.52	53.82	13.32	41.68
KD [16]	47.10	62.17	35.63	56.71	10.09	43.66	44.63	60.98	33.10	55.39	9.33	41.89
FitNet [26]	44.81	59.18	34.41	53.92	13.60	42.42	44.05	58.02	32.50	52.00	12.72	40.28
DKD [19]	47.01	62.53	36.87	57.52	11.74	44.17	46.21	61.42	34.72	55.70	11.41	42.54
ReviewKD [30]	48.71	62.70	38.44	57.78	14.69	44.71	46.67	60.87	36.41	55.56	13.48	42.70
LTKD	54.23	64.21	45.74	59.91	20.57	47.73	54.24	62.90	45.55	58.53	22.72	46.54
Δ	+5.52	+1.51	+7.30	+2.13	+5.88	+3.02	+7.57	+1.48	+9.14	+2.83	+9.24	+3.84

TABLE I: Accuracy (%) on both the tail group classes (\mathcal{T}) and the overall classes (All) in the CIFAR100-LT test sets when using teacher and student models with homogeneous architectures. The best result is highlighted in **bold**, and the second-best result is indicated with underline. Δ denotes the performance gap between the best and the second-best results.

This simple modification ensures that each group contributes equally to the intra-group distillation loss, preventing the overrepresented head group from dominating the learning process.

D. Long-Tailed Knowledge Distillation

We now present our final formulation for Long-Tailed Knowledge Distillation (LTKD), which jointly addresses the two core limitations of conventional KD under long-tailed class distributions: inter-group prediction bias and intra-group imbalance in learning signals.

To mitigate the first issue, we proposed in Sec. III-B a group-level rebalancing mechanism that calibrates the teacher’s inter-group prediction vector \mathbf{p}_G^T toward a uniform distribution across the head, medium, and tail class groups. This produces the rebalanced group-level distribution $\hat{\mathbf{p}}_G^T$, which reduces the overemphasis on head classes and enables fairer supervision.

To address the second issue, we introduced in Sec. III-C a balanced intra-group distillation strategy that eliminates the teacher-weighted terms p_G^T and instead assigns equal importance to the intra-group KL divergences. This ensures that the supervision signal from each group—regardless of its class frequency—is equally reflected during student training.

Combining these two complementary strategies, we define the final LTKD loss as:

$$\text{LTKD} = \alpha \cdot \text{KL}(\hat{\mathbf{p}}_G^T \| \mathbf{p}_G^S) + \beta \cdot \sum_G \text{KL}(\tilde{\mathbf{p}}_G^T \| \tilde{\mathbf{p}}_G^S),$$

where:

- $\hat{\mathbf{p}}_G^T$ and \mathbf{p}_G^S denote the rebalanced inter-group distributions from the teacher and the original distribution from the student, respectively,
- $\tilde{\mathbf{p}}_G^T$ and $\tilde{\mathbf{p}}_G^S$ represent the intra-group normalized distributions within group $G \in \{\mathcal{H}, \mathcal{M}, \mathcal{T}\}$,
- α and β are hyperparameters that balance the contributions of the inter-group and intra-group distillation terms.

This formulation enables the student model to learn from a re-calibrated teacher that delivers fair and balanced supervision across all groups. As we will show in Sec. IV, this unified loss leads to consistent performance improvements—especially for tail classes—demonstrating the effectiveness of LTKD in long-tailed knowledge distillation.

IV. EXPERIMENTS

In this section, we evaluate the effectiveness of the proposed Long-Tailed Knowledge Distillation (LTKD) on three widely used long-tailed benchmarks: CIFAR-100-LT [21], TinyImageNet-LT, ImageNet-LT [22]. We further analyze LTKD through ablation studies on inter-group balancing strategies, individual components, and hyperparameters. Additionally, we present t-SNE visualizations to qualitatively assess the learned feature representations across class groups.

A. Dataset

We construct CIFAR-100-LT, TinyImageNet-LT, and ImageNet-LT by introducing class imbalance into the balanced

T-S Pairs	ResNet32×4 – ShuffleNetV1						VGG13 – MobileNetV2					
γ Group	10		20		100		10		20		100	
	\mathcal{T}	All	\mathcal{T}	All	\mathcal{T}	All	\mathcal{T}	All	\mathcal{T}	All	\mathcal{T}	All
Teacher	50.72	64.95	39.19	58.82	15.28	45.35	45.67	60.77	36.43	55.10	14.01	43.11
Student	40.04	54.06	29.91	48.22	10.74	36.21	30.47	44.58	22.32	39.25	7.04	27.56
KD [16]	47.08	60.88	36.13	55.03	13.07	42.04	39.78	53.64	29.05	47.69	8.99	34.56
FitNet [26]	44.82	58.70	33.77	52.78	13.36	40.66	29.38	43.82	21.38	38.54	7.26	28.31
DKD [19]	<u>50.23</u>	<u>63.32</u>	<u>39.00</u>	<u>57.81</u>	14.98	<u>44.76</u>	<u>41.81</u>	<u>55.84</u>	<u>31.48</u>	<u>50.27</u>	10.94	<u>38.22</u>
ReviewKD [30]	50.02	63.31	38.38	57.64	<u>15.18</u>	44.69	40.03	53.17	29.70	48.06	<u>11.75</u>	36.31
LTKD	54.87	64.60	45.94	59.62	23.93	48.59	46.49	57.18	38.33	52.03	18.24	41.04
Δ	+4.64	+1.28	+6.94	+1.81	+8.75	+3.83	+4.68	+1.34	+6.85	+1.76	+6.49	+2.82
T-S Pairs	WRN-40-2 – ShuffleNetV1						ResNet50 – MobileNetV2					
γ Group	10		20		100		10		20		100	
	\mathcal{T}	All	\mathcal{T}	All	\mathcal{T}	All	\mathcal{T}	All	\mathcal{T}	All	\mathcal{T}	All
Teacher	49.77	63.05	39.88	58.27	14.88	44.78	49.74	63.51	37.74	56.70	14.42	42.26
Student	40.04	54.06	29.91	48.22	10.74	36.21	30.47	44.58	22.32	39.25	7.04	27.56
KD [16]	49.10	62.37	38.30	56.61	12.59	42.56	39.59	53.55	30.22	48.87	10.00	36.17
FitNet [26]	45.02	58.72	34.56	53.40	13.30	41.27	29.40	42.86	21.21	38.22	7.44	28.01
DKD [19]	50.86	63.65	39.94	58.28	15.04	45.24	<u>43.29</u>	<u>57.20</u>	<u>33.23</u>	<u>52.20</u>	<u>12.45</u>	<u>39.21</u>
ReviewKD [30]	<u>51.24</u>	<u>63.90</u>	<u>40.44</u>	<u>58.63</u>	<u>15.81</u>	<u>45.40</u>	33.68	47.75	24.80	42.08	9.75	31.86
LTKD	57.40	65.42	48.42	60.94	23.99	48.60	48.43	57.46	40.82	53.70	21.04	42.45
Δ	+6.16	+1.52	+7.98	+2.31	+8.18	+3.20	+5.14	+0.26	+7.59	+1.50	+8.59	+3.24

TABLE II: Accuracy (%) on both the tail group classes (\mathcal{T}) and the overall classes (All) in the CIFAR100-LT test sets when using teacher and student models with heterogeneous architectures. The best result is highlighted in **bold**, and the second-best result is indicated with underline. Δ denotes the performance gap between the best and the second-best results.

CIFAR-100 [17], TinyImageNet [18], and ImageNet [39] datasets, following previous works [21], [22], [40]. The balanced CIFAR-100 consists of 100 categories with 50,000 training and 10,000 test images, each of size 32×32 pixels. TinyImageNet is a subset of ImageNet comprising 200 categories, with each class containing 500 training and 50 test images, resized to 64×64 pixels. ImageNet consists of 1.28 million training images and 5,000 test images across 1,000 categories, each resized to 224×224 pixels.

For each class c , the number of training samples, denoted by $|\mathcal{D}_c|$, is reduced using an exponential decay function:

$$|\hat{\mathcal{D}}| = |\mathcal{D}_c| \cdot \gamma^{-c/C},$$

where C is the total number of classes and γ is the imbalance factor. The test set remains balanced to ensure fair evaluation. The imbalance factor γ is defined as the ratio between the number of training samples in the largest and smallest classes [21]. For both CIFAR-100-LT and TinyImageNet-LT, we construct three versions of the training set with imbalance factors of [10, 20, 100]. For ImageNet-LT, imbalance factors of [5, 10, 20] are used.

B. Implementation Details

To verify the effectiveness of the proposed method across various teacher-student pairs, we conduct experiments using widely used convolutional neural network architectures, including ResNet [1], VGG [2], WideResNet (WRN) [41],

ShuffleNet [42], [43], and MobileNet [44]. We consider both homogeneous settings, where the teacher and student share the same backbone architecture, and heterogeneous settings, where they use different backbones. The optimization is performed using stochastic gradient descent with a momentum of 0.9 and a weight decay of 5×10^{-4} .

Our methods are compared against various existing techniques, including representative logit-based methods such as KD and DKD, as well as feature-based methods like FitNet and ReviewKD. *Each experiment is conducted three times, and the average performance is reported.*

C. Main Results

We evaluate the effectiveness of LTKD across multiple teacher-student architecture pairs and varying degrees of class imbalance. The results are reported for both the tail-class accuracy (\mathcal{T}) and the overall classification accuracy (All), with comparisons to existing state-of-the-art KD methods including KD, FitNet, DKD, and ReviewKD.

1) *CIFAR100-LT*: Table I and Table II present the performance of LTKD under homogeneous and heterogeneous teacher-student configurations, respectively. Across all settings, LTKD consistently surpasses prior methods, showing remarkable improvements on both overall and tail-class accuracy.

In particular, under a ResNet32×4–ResNet8×4 pair with an imbalance factor of 100, LTKD improves the tail-class

T-S Pairs	ResNet32×4 – ResNet8×4						VGG13 – VGG8					
γ Group	10		20		100		10		20		100	
	\mathcal{T}	All	\mathcal{T}	All	\mathcal{T}	All	\mathcal{T}	All	\mathcal{T}	All	\mathcal{T}	All
Teacher	38.47	52.64	28.74	47.49	9.53	35.37	32.53	45.23	21.85	39.75	6.29	29.71
Student	29.72	44.60	21.46	40.25	4.73	30.62	31.12	43.76	22.19	39.00	6.88	29.96
KD [16]	27.34	45.38	18.11	41.35	3.38	31.42	31.92	47.16	20.60	41.49	3.99	30.95
FitNet [26]	29.65	44.64	20.86	40.24	5.51	30.66	32.04	44.43	23.43	39.47	6.87	30.09
DKD [19]	<u>34.70</u>	48.93	<u>26.58</u>	<u>44.84</u>	<u>9.09</u>	<u>34.61</u>	33.20	<u>48.01</u>	22.65	<u>42.44</u>	5.88	31.82
ReviewKD [30]	32.85	<u>49.13</u>	23.43	44.62	5.39	33.51	<u>34.39</u>	47.66	<u>24.84</u>	42.36	<u>7.61</u>	<u>32.18</u>
LTKD	40.66	51.33	31.33	47.05	10.48	36.21	38.90	49.43	29.30	44.22	9.73	33.78
Δ	+5.96	+2.20	+4.75	+2.21	+1.39	+1.60	+4.51	+1.42	+4.46	+1.78	+2.12	+1.60
T-S Pairs	WRN-40-2 – WRN-40-1						ResNet110 – ResNet32					
γ Group	10		20		100		10		20		100	
	\mathcal{T}	All	\mathcal{T}	All	\mathcal{T}	All	\mathcal{T}	All	\mathcal{T}	All	\mathcal{T}	All
Teacher	34.21	49.09	23.50	44.15	6.05	33.66	32.78	47.01	23.36	42.08	6.31	32.11
Student	28.97	44.34	20.27	40.16	4.79	30.31	28.54	44.02	20.45	40.10	4.61	30.47
KD [16]	27.35	45.72	17.12	40.67	2.82	31.59	28.87	45.47	19.77	40.60	3.87	30.86
FitNet [26]	28.85	44.25	20.02	39.92	3.74	29.98	28.51	43.52	20.31	39.12	4.97	29.86
DKD [19]	31.92	47.32	21.52	42.83	5.08	33.04	31.26	46.79	22.06	42.03	5.32	32.09
ReviewKD [30]	<u>33.53</u>	<u>48.56</u>	<u>24.00</u>	<u>43.71</u>	<u>5.84</u>	<u>33.15</u>	<u>31.80</u>	<u>47.21</u>	<u>22.33</u>	<u>42.47</u>	<u>5.36</u>	<u>32.23</u>
LTKD	36.55	48.86	27.70	44.49	8.91	34.80	37.19	47.85	29.08	43.68	9.68	33.80
Δ	+3.02	+0.30	+3.70	+0.78	+3.07	+1.65	+5.39	+0.64	+6.75	+1.21	+4.32	+1.57

TABLE III: Accuracy (%) on both the tail group classes (\mathcal{T}) and the overall classes (All) in the TinyImageNet-LT test sets when using teacher and student models with homogeneous architectures. The best result is highlighted in **bold**, and the second-best result is indicated with underline. Δ denotes the performance gap between the best and the second-best results.

accuracy from 15.09% (ReviewKD) to 27.21%, and overall accuracy from 45.91% to 51.08%. Similar gains are observed across other imbalance levels and architecture combinations. Notably, even in the most challenging settings (e.g., VGG13–MobileNetV2, $\gamma = 100$), LTKD achieves a substantial improvement of +6.49% in tail accuracy and +2.82% in overall accuracy.

These results demonstrate that LTKD not only enhances performance for underrepresented classes but also improves generalization across the full label space, validating the importance of decomposed and rebalanced supervision.

2) *TinyImageNet-LT*: The results on TinyImageNet-LT (Tables III and IV) further confirm the efficacy of LTKD. Compared to other methods, LTKD achieves superior performance across all imbalance levels and teacher-student pairs.

For example, in the ResNet32×4–ResNet8×4 setting with $\gamma = 100$, LTKD improves tail accuracy from 9.09% (DKD) to 10.48%, and overall accuracy from 34.61% to 36.21%. In more resource-constrained settings like VGG13–MobileNetV2, LTKD lifts the tail-class accuracy from 7.02% (ReviewKD) to 9.52%, and overall accuracy from 29.97% (DKD) to 32.30%.

Moreover, the improvements in tail-class performance are particularly significant in heterogeneous setups, highlighting LTKD’s strength in effectively transferring knowledge from a biased teacher to a compact student across varying architectural capacities.

3) *ImageNet-LT*: To validate the scalability and generality of our method, we further evaluate LTKD on the large-scale ImageNet-LT benchmark. LTKD consistently outperforms all compared methods across varying imbalance factors ($\gamma \in \{5, 10, 20\}$) and different teacher–student architectures.

In the ResNet34–ResNet18 configuration, LTKD improves tail accuracy by +1.06%, +1.75%, and +2.40% for $\gamma = 5, 10, 20$, respectively, compared to the best existing method. This trend remains consistent in the ResNet50–MobileNetV1 setting, where LTKD achieves up to +3.20% improvement on tail classes and also delivers gains in overall accuracy.

These results highlight the method’s ability to perform effective and balanced knowledge transfer even under severe real-world imbalance.

D. Ablation Study

To better understand the effectiveness of the proposed LTKD framework, we perform a detailed ablation study on CIFAR-100-LT with an imbalance factor of 20. Specifically, we investigate the effects of (1) rebalancing the inter-group prediction distribution and (2) uniformly weighting intra-group losses. In addition, we analyze the sensitivity of LTKD to its hyperparameters α and β , which control the relative importance of the inter- and intra-group terms. The results are reported in terms of tail-class accuracy (\mathcal{T}) and overall accuracy (All).

T-S Pairs	ResNet32×4 – ShuffleNetV1						VGG13 – MobileNetV2					
γ Group	10		20		100		10		20		100	
	\mathcal{T}	All	\mathcal{T}	All	\mathcal{T}	All	\mathcal{T}	All	\mathcal{T}	All	\mathcal{T}	All
Teacher	38.47	52.64	28.74	47.49	9.53	35.37	32.53	45.23	21.85	39.75	6.29	29.71
Student	24.43	37.10	16.80	31.85	4.71	22.77	26.98	39.73	17.38	33.14	3.97	22.99
KD [16]	34.67	49.05	24.12	42.81	5.62	30.74	31.24	45.60	19.53	39.50	3.27	28.44
FitNet [26]	25.23	36.79	16.39	32.04	4.84	23.17	25.81	37.98	16.51	31.90	4.07	22.71
DKD [19]	<u>36.83</u>	<u>50.22</u>	26.64	44.38	8.34	<u>33.23</u>	<u>33.07</u>	<u>46.79</u>	22.06	<u>40.87</u>	5.70	<u>29.97</u>
ReviewKD [30]	36.30	49.27	<u>27.09</u>	<u>44.72</u>	<u>8.49</u>	33.12	32.37	44.99	<u>22.77</u>	39.36	<u>7.02</u>	29.20
LTKD	42.12	51.64	33.06	46.41	12.85	35.09	39.04	48.71	28.28	43.22	9.52	32.30
Δ	+5.29	+1.42	+5.97	+1.69	+4.36	+1.86	+5.97	+1.92	+5.51	+2.35	+2.50	+2.33

T-S Pairs	WRN-40-2 – ShuffleNetV1						ResNet50 – MobileNetV2					
γ Group	10		20		100		10		20		100	
	\mathcal{T}	All	\mathcal{T}	All	\mathcal{T}	All	\mathcal{T}	All	\mathcal{T}	All	\mathcal{T}	All
Teacher	34.21	49.09	23.50	44.15	6.05	33.66	39.43	52.86	29.37	46.36	10.71	35.49
Student	24.43	37.10	16.80	31.85	4.71	22.77	26.98	39.73	17.38	33.14	3.97	22.99
KD [16]	32.28	47.64	21.72	42.54	4.64	32.09	34.09	48.70	23.33	42.23	5.49	30.23
FitNet [26]	24.48	36.57	16.59	31.59	5.03	23.02	25.66	38.16	16.53	32.07	4.00	22.29
DKD [19]	34.45	48.68	23.40	43.78	6.55	33.25	<u>37.07</u>	<u>50.37</u>	<u>27.11</u>	<u>44.30</u>	<u>8.56</u>	<u>33.01</u>
ReviewKD [30]	<u>35.89</u>	<u>48.94</u>	<u>26.54</u>	<u>43.93</u>	<u>8.67</u>	<u>33.61</u>	30.26	42.84	20.97	36.99	5.50	26.67
LTKD	39.66	50.19	30.05	45.58	11.13	35.39	42.59	51.95	31.95	45.66	11.97	34.60
Δ	+3.77	+1.25	+3.51	+1.65	+2.46	+1.78	+5.52	+1.58	+4.84	+1.36	+3.41	+1.59

TABLE IV: Accuracy (%) on both the tail group classes (\mathcal{T}) and the overall classes (All) in the TinyImageNet-LT test sets when using teacher and student models with heterogeneous architectures. The best result is highlighted in **bold**, and the second-best result is indicated with underline. Δ denotes the performance gap between the best and the second-best results.

T-S Pairs	ResNet34 – ResNet18						ResNet50 – MobileNetV1					
γ Group	5		10		20		5		10		20	
	\mathcal{T}	All	\mathcal{T}	All	\mathcal{T}	All	\mathcal{T}	All	\mathcal{T}	All	\mathcal{T}	All
Teacher	57.75	67.61	50.61	63.85	43.00	59.91	59.62	69.06	52.69	65.57	44.82	61.46
Student	54.48	64.73	47.45	61.18	39.98	57.25	55.42	65.46	49.49	62.55	41.68	58.94
KD [16]	56.14	66.27	49.35	63.03	41.72	59.15	56.58	66.51	50.42	63.70	42.45	59.91
DKD [19]	56.83	66.84	49.95	63.50	42.65	59.82	58.54	68.09	52.39	65.04	45.04	61.46
ReviewKD [30]	<u>57.27</u>	<u>66.96</u>	<u>50.80</u>	<u>63.72</u>	<u>43.48</u>	<u>60.15</u>	<u>58.59</u>	<u>68.10</u>	<u>53.06</u>	<u>65.31</u>	<u>45.35</u>	<u>61.84</u>
LTKD	58.33	67.23	52.55	64.29	45.88	60.80	60.17	68.48	54.40	65.52	48.55	62.22
Δ	+1.06	+0.27	+1.75	+0.57	+2.40	+0.65	+1.58	+0.38	+1.34	+0.21	+3.20	+0.38

TABLE V: Accuracy (%) on both the tail group classes (\mathcal{T}) and the overall classes (All) in the ImageNet-LT test sets. The best result is highlighted in **bold**, and the second-best result is indicated with underline. Δ denotes the performance gap between the best and the second-best results.

1) *Effectiveness of Inter-Group Balancing*: In this experiment, we isolate the impact of the proposed inter-group balancing strategy by comparing it against a baseline that applies inter-group distillation without any correction. In both settings, the intra-group loss is disabled to ensure a fair comparison.

As shown in Table VI, applying our inter-group balancing leads to consistent gains in tail-class accuracy across all teacher-student pairs. For example, in the ResNet32×4-ResNet8×4 setting, tail accuracy improves from 38.30% to 40.51%, and overall accuracy increases by +0.79%.

Similar improvements are observed in VGG13-MobileNetV2 and WRN-40-2-ShuffleNetV1 settings, demonstrating the effectiveness of our strategy in promoting better performance on underrepresented classes.

Interestingly, in the ResNet32×4-ShuffleNetV1 configuration, our method also achieves a tail-class accuracy improvement from 30.01% to 30.68%. However, the overall accuracy experiences a marginal drop (from 48.82% to 48.81%), which deviates slightly from the trends observed in other teacher-student pairs. Further analysis reveals that this minor decrease is caused by a small performance degradation on

Models	Teacher Student		ResNet32×4				VGG13				WRN-40-2			
			ResNet8×4		ShuffleNetV1		VGG8		MobileNetV2		WRN-40-1		ShuffleNetV1	
Loss	Inter	Intra	\mathcal{T}	All	\mathcal{T}	All	\mathcal{T}	All	\mathcal{T}	All	\mathcal{T}	All	\mathcal{T}	All
Biased	✓	✗	38.30	55.77	30.01	48.82	35.55	53.30	23.42	40.29	34.64	53.97	30.23	49.31
Ours	✓	✗	40.51	56.55	30.68	48.81	37.26	53.70	23.97	40.30	35.23	54.35	32.44	49.91
Δ			+2.21	+0.78	+0.67	-0.01	+1.71	+0.40	+0.55	+0.01	+0.59	+0.38	+2.21	+0.60

TABLE VI: Performance comparison of inter-group distillation strategies on CIFAR-100-LT with an imbalance factor of 20. “Biased” refers to using the original inter-group distillation loss without balancing, while “Ours” applies the proposed balanced inter-group loss. Intra-group loss is not used in this setting. \mathcal{T} denotes tail-class accuracy, and All indicates overall accuracy. The last row (Δ) shows the improvement of our method over the Biased baseline.

Models	Teacher Student		ResNet32×4				VGG13				WRN-40-2			
			ResNet8×4		ShuffleNetV1		VGG8		MobileNetV2		WRN-40-1		ShuffleNetV1	
Loss	Inter	Intra	\mathcal{T}	All	\mathcal{T}	All	\mathcal{T}	All	\mathcal{T}	All	\mathcal{T}	All	\mathcal{T}	All
Baseline	✓	✓	36.81	57.41	36.13	55.03	37.29	56.13	29.05	47.69	35.63	56.71	38.30	56.61
	✓	✗	40.51	56.55	30.68	48.81	37.26	53.70	23.97	40.30	35.23	54.35	32.44	49.91
Ours	✗	✓	42.34	59.78	39.10	56.84	38.54	56.83	31.99	49.20	39.67	58.11	40.45	57.65
	✓	✓	49.70	62.54	45.94	59.62	45.77	58.86	38.33	52.03	45.74	59.91	48.42	60.94

TABLE VII: Ablation study of the proposed inter-group and intra-group distillation losses on CIFAR-100-LT with an imbalance factor of 20. “Baseline” corresponds to vanilla KD using the original (biased) teacher outputs with no correction. “Ours (Inter only)” applies only the proposed inter-group balancing method. “Ours (Intra only)” uses only the uniform intra-group weighting strategy. “Ours (Inter + Intra)” combines both inter-group and intra-group adjustments, yielding the best performance across all teacher–student pairs. \mathcal{T} denotes tail-class accuracy, and All denotes overall accuracy.

head classes, likely due to the suppression of dominant group signals during the inter-group rebalancing process.

Nevertheless, we find that this issue can be fully addressed by incorporating the intra-group loss. When intra-group supervision is added (see Table VII, “Ours (Inter + Intra)” row), the model not only recovers but significantly surpasses the baseline in both tail and overall accuracy, achieving 45.94% and 59.62%, respectively. This result confirms that inter-group balancing is a powerful and generalizable strategy when used in conjunction with complementary intra-group component.

2) *Impact of Each Component in LTKD*: Next, we perform a comprehensive ablation to disentangle the individual contributions of the inter-group and intra-group components in LTKD. As summarized in Table VII, we consider four variants: Baseline, Inter only, Intra only, and Both.

We observe that each component independently improves both tail and overall accuracy. Specifically, adding the inter-group loss leads to a +7.36% improvement in tail accuracy, while incorporating the intra-group loss yields an even larger gain of +9.19% (e.g., for the ResNet32×4–ResNet8×4 pair). This demonstrates that uniformly weighting intra-group losses is particularly effective in mitigating teacher bias in long-tailed prediction distributions. The best performance is consistently achieved when both strategies are combined. For example, in the VGG13–MobileNetV2 setting, the full LTKD improves tail accuracy by +9.28% and overall accuracy by +4.34% over the baseline. This trend holds across all architecture combinations, confirming that the two strategies are complementary and synergistic.

These findings underscore the importance of jointly addressing both inter-group and intra-group biases in long-tailed

knowledge distillation, and validate the design of our LTKD framework.

3) *Hyperparameters*: To investigate the sensitivity of LTKD to its hyperparameters, we conduct experiments by varying the inter-group loss weight α and the intra-group loss weight β individually. We fix the teacher–student pair to ResNet32×4 and ResNet8×4 on CIFAR-100-LT with an imbalance factor of 20.

We first fix $\beta = 1$ and vary $\alpha \in \{1, 2, 4, 6, 8, 10\}$. As shown in Fig. 4 (Top), the overall accuracy gradually improves with increasing α , peaking at $\alpha = 6$ (61.45%). Beyond this point, performance slightly degrades, suggesting that overly emphasizing the inter-group term may lead to suboptimal generalization. Next, we fix $\alpha = 6$ and vary $\beta \in \{1, 2, 4, 6, 8, 10\}$. Accuracy continues to increase and reaches the highest value of 62.54% at $\beta = 6$. Importantly, LTKD consistently outperforms ReviewKD (59.17%)—the best-performing previous method in Table I—across a wide range of hyperparameter settings. This demonstrates the robustness of LTKD in terms of its balancing components and validates the effectiveness of our reformulation.

We also observe similar trends for the tail-class accuracy, reported in Fig. 4 (Bottom). When $\beta = 1$ is fixed, tail accuracy peaks at $\alpha = 2$ with 48.04%, then slightly declines. When fixing $\alpha = 6$ and varying β , tail accuracy steadily improves, reaching 49.72% at $\beta = 8$. This represents a significant gain of +9.6% over ReviewKD (40.12%) on tail classes, indicating that LTKD is not only effective for overall accuracy but also particularly beneficial for underrepresented classes under long-tailed distributions.

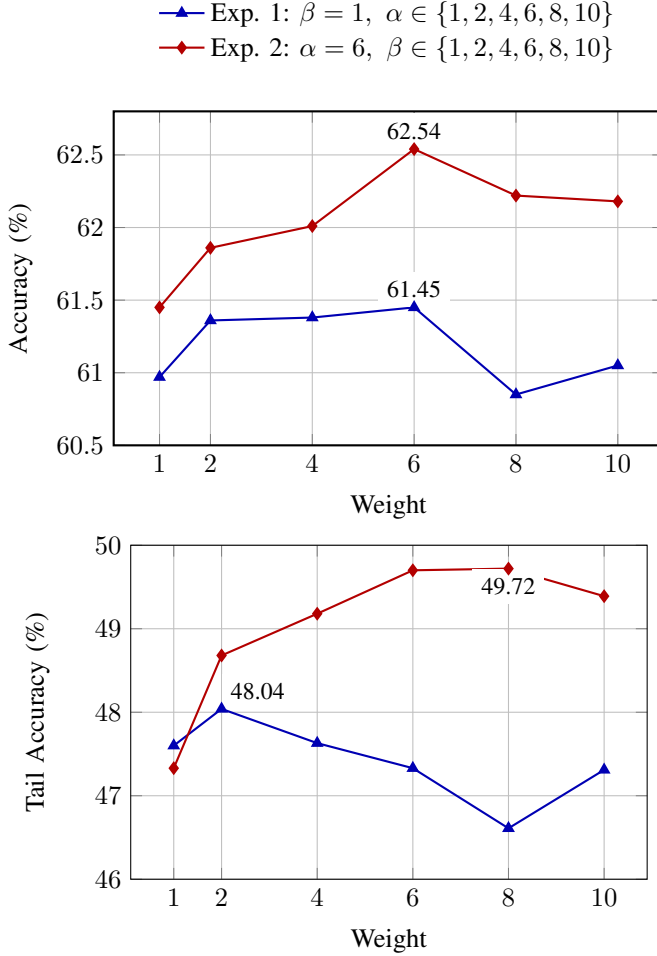


Fig. 4: Ablation study on the hyperparameters α and β in LTKD on CIFAR-100-LT (imbalance factor = 20). Top: overall accuracy. Bottom: tail-class accuracy (\mathcal{T}). The blue line shows results when the intra-group loss weight (β) is fixed to 1 and the inter-group loss weight (α) is varied. The red line shows results when α is fixed to 6 and β is varied.

E. tSNE Visualization

To further investigate the quality of the learned representations, we visualize the feature embeddings of the student model (ShuffleNetV1) trained from the teacher model (ResNet32x4) using both KD and our proposed LTKD. Fig. 5 shows the 2D projection of features from the CIFAR-100-LT validation set, where each point is colored according to its class group: head (red), medium (green), or tail (blue). In the KD case (Fig. 5a), the embeddings of tail-class samples appear scattered and poorly separated, indicating suboptimal feature learning for underrepresented classes. In contrast, LTKD (Fig. 5b) produces tighter and more distinct clusters, especially for the tail group. This result supports our claim that rebalancing inter-group and intra-group knowledge transfer enables the student to learn richer and more discriminative representations, particularly for tail-class groups.

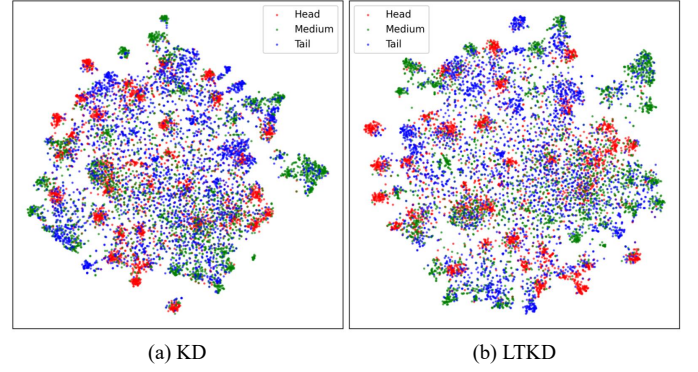


Fig. 5: t-SNE visualization of student feature representations. (a) Student trained with standard KD. (b) Student trained with our proposed LTKD. Points are colored by class group: head (red), medium (green), and tail (blue). Compared to KD, LTKD yields more compact and well-separated clusters for tail classes.

V. CONCLUSION

In this work, we addressed a key limitation of knowledge distillation in long-tailed visual recognition: the ineffective transfer of knowledge from a teacher model biased by class imbalance. To tackle this, we proposed Long-Tailed Knowledge Distillation (LTKD), a novel framework that decomposes the KD objective into inter-group and intra-group KL divergence terms. This formulation enables explicit analysis and correction of structural biases in the teacher’s predictions. To mitigate inter-group bias, we introduced a rebalancing mechanism that calibrates the group-wise prediction distribution. For intra-group supervision, we employed a uniform weighting strategy to ensure fair learning across all class groups, regardless of their sample frequency. Extensive experiments on CIFAR-100-LT, TinyImageNet-LT, ImageNet-LT demonstrate that both components contribute significantly to improved performance. Notably, LTKD consistently enhances tail-class accuracy and, in many cases, even surpasses the teacher’s performance. These findings suggest that decomposing and rebalancing the distillation process is crucial for mitigating teacher bias and building more robust student models under long-tailed distributions. Future work includes extending this decomposition framework to other domains such as object detection and semantic segmentation, where long-tail issues are also pervasive.

REFERENCES

- [1] K. He, X. Zhang, S. Ren, and J. Sun, “Deep residual learning for image recognition,” in *Proceedings of the IEEE conference on computer vision and pattern recognition*, pp. 770–778, 2016.
- [2] K. Simonyan and A. Zisserman, “Very deep convolutional networks for large-scale image recognition,” in *ICLR*, May 2015.
- [3] A. Dosovitskiy, L. Beyer, A. Kolesnikov, D. Weissenborn, X. Zhai, T. Unterthiner, M. Dehghani, M. Minderer, G. Heigold, S. Gelly, *et al.*, “An image is worth 16x16 words: Transformers for image recognition at scale,” *arXiv preprint arXiv:2010.11929*, 2020.
- [4] J. Redmon, S. Divvala, R. Girshick, and A. Farhadi, “You only look once: Unified, real-time object detection,” in *Proceedings of the IEEE conference on computer vision and pattern recognition*, pp. 779–788, 2016.

- [5] S. Ren, K. He, R. Girshick, and J. Sun, "Faster r-cnn: Towards real-time object detection with region proposal networks," *Advances in neural information processing systems*, vol. 28, 2015.
- [6] J. Long, E. Shelhamer, and T. Darrell, "Fully convolutional networks for semantic segmentation," in *Proceedings of the IEEE conference on computer vision and pattern recognition*, pp. 3431–3440, 2015.
- [7] H. Zhao, J. Shi, X. Qi, X. Wang, and J. Jia, "Pyramid scene parsing network," in *Proceedings of the IEEE conference on computer vision and pattern recognition*, pp. 2881–2890, 2017.
- [8] L.-C. Chen, G. Papandreou, I. Kokkinos, K. Murphy, and A. L. Yuille, "DeepLab: Semantic image segmentation with deep convolutional nets, atrous convolution, and fully connected crfs," *IEEE transactions on pattern analysis and machine intelligence*, vol. 40, no. 4, pp. 834–848, 2017.
- [9] D. Wu, M.-W. Liao, W.-T. Zhang, X.-G. Wang, X. Bai, W.-Q. Cheng, and W.-Y. Liu, "Yolop: You only look once for panoptic driving perception," *Machine Intelligence Research*, vol. 19, no. 6, pp. 550–562, 2022.
- [10] C. Han, Q. Zhao, S. Zhang, Y. Chen, Z. Zhang, and J. Yuan, "Yolopv2: Better, faster, stronger for panoptic driving perception," *arXiv preprint arXiv:2208.11434*, 2022.
- [11] A. Prakash, K. Chitta, and A. Geiger, "Multi-modal fusion transformer for end-to-end autonomous driving," in *Proceedings of the IEEE/CVF conference on computer vision and pattern recognition*, pp. 7077–7087, 2021.
- [12] Y. Xiao, F. Codevilla, A. Gurram, O. Urfalioglu, and A. M. López, "Multimodal end-to-end autonomous driving," *IEEE Transactions on Intelligent Transportation Systems*, vol. 23, no. 1, pp. 537–547, 2020.
- [13] J. Liu, B. Zhuang, Z. Zhuang, Y. Guo, J. Huang, J. Zhu, and M. Tan, "Discrimination-aware network pruning for deep model compression," *IEEE Transactions on Pattern Analysis and Machine Intelligence*, vol. 44, no. 8, pp. 4035–4051, 2021.
- [14] Y. Zhou, S.-M. Moosavi-Dezfooli, N.-M. Cheung, and P. Frossard, "Adaptive quantization for deep neural network," in *Proceedings of the AAAI Conference on Artificial Intelligence*, vol. 32, 2018.
- [15] J. Gou, B. Yu, S. J. Maybank, and D. Tao, "Knowledge distillation: A survey," *International Journal of Computer Vision*, vol. 129, pp. 1789–1819, 2021.
- [16] G. Hinton, O. Vinyals, and J. Dean, "Distilling the knowledge in a neural network," *arXiv preprint arXiv:1503.02531*, 2015.
- [17] A. Krizhevsky, G. Hinton, *et al.*, "Learning multiple layers of features from tiny images," 2009.
- [18] Y. Le and X. Yang, "Tiny imagenet visual recognition challenge," *CS 231N*, vol. 7, no. 7, p. 3, 2015.
- [19] B. Zhao, Q. Cui, R. Song, Y. Qiu, and J. Liang, "Decoupled knowledge distillation," in *Proceedings of the IEEE/CVF Conference on computer vision and pattern recognition*, pp. 11953–11962, 2022.
- [20] Y. Zhang, B. Kang, B. Hooi, S. Yan, and J. Feng, "Deep long-tailed learning: A survey," *IEEE transactions on pattern analysis and machine intelligence*, vol. 45, no. 9, pp. 10795–10816, 2023.
- [21] Y. Cui, M. Jia, T.-Y. Lin, Y. Song, and S. Belongie, "Class-balanced loss based on effective number of samples," in *Proceedings of the IEEE/CVF conference on computer vision and pattern recognition*, pp. 9268–9277, 2019.
- [22] Z. Liu, Z. Miao, X. Zhan, J. Wang, B. Gong, and S. X. Yu, "Large-scale long-tailed recognition in an open world," in *Proceedings of the IEEE/CVF conference on computer vision and pattern recognition*, pp. 2537–2546, 2019.
- [23] S. Kim, G. Ham, Y. Cho, and D. Kim, "Robustness-reinforced knowledge distillation with correlation distance and network pruning," *IEEE Transactions on Knowledge and Data Engineering*, 2024.
- [24] Y. Zhang, T. Xiang, T. M. Hospedales, and H. Lu, "Deep mutual learning," in *Proceedings of the IEEE Conference on Computer Vision and Pattern Recognition*, pp. 4320–4328, 2018.
- [25] S. I. Mirzadeh, M. Farajtabar, A. Li, N. Levine, A. Matsukawa, and H. Ghasemzadeh, "Improved knowledge distillation via teacher assistant," in *AAAI*, 2020.
- [26] A. Romero, N. Ballas, S. E. Kahou, A. Chassang, C. Gatta, and Y. Bengio, "Fitnets: Hints for thin deep nets," *arXiv preprint arXiv:1412.6550*, 2014.
- [27] S. Zagoruyko and N. Komodakis, "Paying more attention to attention: Improving the performance of convolutional neural networks via attention transfer," *arXiv preprint arXiv:1612.03928*, 2016.
- [28] W. Park, D. Kim, Y. Lu, and M. Cho, "Relational knowledge distillation," in *Proceedings of the IEEE/CVF Conference on Computer Vision and Pattern Recognition*, pp. 3967–3976, 2019.
- [29] Y. Tian, D. Krishnan, and P. Isola, "Contrastive representation distillation," *arXiv preprint arXiv:1910.10699*, 2019.
- [30] P. Chen, S. Liu, H. Zhao, and J. Jia, "Distilling knowledge via knowledge review," in *Proceedings of the IEEE/CVF Conference on Computer Vision and Pattern Recognition*, pp. 5008–5017, 2021.
- [31] Z. Guo, H. Yan, H. Li, and X. Lin, "Class attention transfer based knowledge distillation," in *Proceedings of the IEEE/CVF Conference on Computer Vision and Pattern Recognition*, pp. 11868–11877, 2023.
- [32] T. Huang, Y. Zhang, M. Zheng, S. You, F. Wang, C. Qian, and C. Xu, "Knowledge diffusion for distillation," *Advances in Neural Information Processing Systems*, vol. 36, pp. 65299–65316, 2023.
- [33] Y. Zhang, T. Huang, J. Liu, T. Jiang, K. Cheng, and S. Zhang, "Freekd: Knowledge distillation via semantic frequency prompt," in *Proceedings of the IEEE/CVF Conference on Computer Vision and Pattern Recognition*, pp. 15931–15940, 2024.
- [34] S. Kim, G. Ham, S. Lee, D. Jang, and D. Kim, "Maximizing discrimination capability of knowledge distillation with energy function," *Knowledge-Based Systems*, vol. 296, p. 111911, 2024.
- [35] S. Kim, "Figkd: Fine-grained knowledge distillation via high-frequency detail transfer," *arXiv preprint arXiv:2505.11897*, 2025.
- [36] S. Alshammari, Y.-X. Wang, D. Ramanan, and S. Kong, "Long-tailed recognition via weight balancing," in *Proceedings of the IEEE/CVF conference on computer vision and pattern recognition*, pp. 6897–6907, 2022.
- [37] S. Zhang, C. Chen, X. Hu, and S. Peng, "Balanced knowledge distillation for long-tailed learning," *Neurocomputing*, vol. 527, pp. 36–46, 2023.
- [38] L. Xiang, G. Ding, and J. Han, "Learning from multiple experts: Self-paced knowledge distillation for long-tailed classification," in *Computer Vision—ECCV 2020: 16th European Conference, Glasgow, UK, August 23–28, 2020, Proceedings, Part V 16*, pp. 247–263, Springer, 2020.
- [39] O. Russakovsky, J. Deng, H. Su, J. Krause, S. Satheesh, S. Ma, Z. Huang, A. Karpathy, A. Khosla, M. Bernstein, *et al.*, "Imagenet large scale visual recognition challenge," *International journal of computer vision*, vol. 115, pp. 211–252, 2015.
- [40] F. Du, P. Yang, Q. Jia, F. Nan, X. Chen, and Y. Yang, "Global and local mixture consistency cumulative learning for long-tailed visual recognitions," in *Proceedings of the IEEE/CVF conference on computer vision and pattern recognition*, pp. 15814–15823, 2023.
- [41] S. Zagoruyko and N. Komodakis, "Wide residual networks," in *BMVC*, 2016.
- [42] X. Zhang, X. Zhou, M. Lin, and J. Sun, "Shufflenet: An extremely efficient convolutional neural network for mobile devices," in *Proceedings of the IEEE conference on computer vision and pattern recognition*, pp. 6848–6856, 2018.
- [43] N. Ma, X. Zhang, H.-T. Zheng, and J. Sun, "Shufflenet v2: Practical guidelines for efficient cnn architecture design," in *Proceedings of the European conference on computer vision (ECCV)*, pp. 116–131, 2018.
- [44] M. Sandler, A. Howard, M. Zhu, A. Zhmoginov, and L.-C. Chen, "MobilenetV2: Inverted residuals and linear bottlenecks," in *CVPR*, 2018.